THE BELL SYSTEM TECHNICAL JOURNAL
Vol. 62, No. 7, September 1983
Printed in U.S.A.

A Comparison of Line Difference Predictions for Time-Frequency Multiplexing of Television Signals

By R. L. SCHMIDT*

(Manuscript received January 27, 1983)

Studies are presented of a scheme utilizing time-frequency multiplexing (TFM) to multiplex two television signals on a microwave radio channel. This scheme transmits alternate lines of the television signal at full bandwidth, along with a differential signal for the remaining lines. The differential signal is derived by subtracting the true value of each picture element from a prediction for that value based on surrounding elements located in the transmitted lines. This differential signal is then placed on a carrier, and frequency multiplexed with the baseband signal. In this way, two television lines of information can be transmitted in one line time, allowing a second similarly constructed signal to be transmitted during the vacated line. Thus, the television signals will be time interleaved on a line-to-line basis. This paper describes the comparison of two different prediction algorithms used to construct the line-differential signal. Time and frequency domain analyses were carried out on the computer and then verified with hardware testing.

I. INTRODUCTION

Recently, a time-frequency multiplexing (TFM) system was described[1] as a method for multiplexing two National Television System Committee (NTSC) color television signals onto a single microwave radio channel. This system proposes to transmit alternate

* Bell Laboratories.

lines of a television signal at full bandwidth, and the remaining lines by means of a band-limited line-differential signal formed by using a prediction obtained from adjacent, full bandwidth lines. This differential signal is then placed on a carrier and frequency multiplexed with a full bandwidth television line. In this way two lines are sent in one line period, and, by time multiplexing, two pictures can be sent on a single microwave radio channel.

The reconstructed picture in the receiver is then a combination of alternate lines of full bandwidth video, and lines regenerated from the prediction and the band-limited line-differential signal. Consequently, a more accurate prediction would require less differential signal information. Stated another way, better picture quality can be attained for a given bandwidth limitation of the differential signal. The proposed differential signal band limiting for the TFM system is 3 MHz, and, within this constraint, an improved prediction would allow the transmission of more detailed pictures.

The originally proposed system had a prediction based on an average of adjacent picture elements of the same color subcarrier phase, from the previous and upcoming lines (Fig. 1). These elements were chosen because we did not have to take into account the color subcarrier, making this prediction the simplest to implement. However, since the prediction elements had to be of the same color subcarrier phase, they were not the elements closest to the element being predicted. This would create a larger differential signal on sharp vertical edges. This paper refers to this prediction as XP_1, and its associated differential signal as $XDIF_1$.

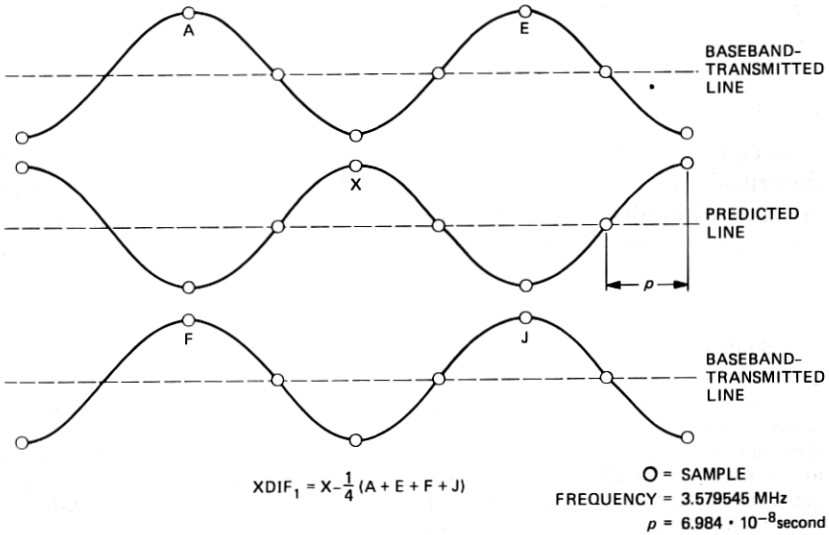

Fig. 1—Derivation of $XDIF_1$ from XP_1 prediction algorithm.

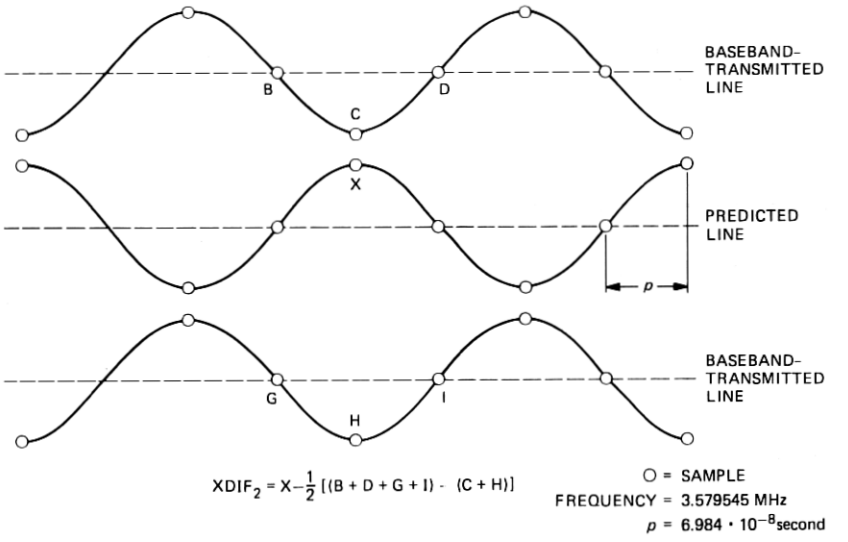

Fig. 2—Derivation of $XDIF_2$ from XP_2 prediction algorithm.

It was conjectured that picture quality would improve if we chose a line difference prediction that used the picture elements from the previous and upcoming lines closer to the coded element (Fig. 2), thus improving the resolution of the predicted value on vertical edges. Here we refer to this prediction as XP_2 and its associated differential signal as $XDIF_2$.

II. TIME DOMAIN ANALYSIS

The complexity of the baseband signal, and its quasi-periodic nature, would make analysis of the network response to an average video signal tedious and not very informative. However, since line-to-line correlation is high, some typical waveforms can be looked at and yield useful results.

Since there is a high content of color subcarrier in a typical television waveform, the differential signal should be small for that frequency. This criterion is met for both line difference predictions, and is shown in Appendix A to be zero for any flat field of constant color.

Appendix B shows that if there is color change from one line to the next the worst case differential signal will be the same for both predictions, with the amplitude being an average of the amplitudes of the two color sine waves for the adjacent lines. However, the worst case for each predictor does not occur at the same color subcarrier phase angle.

Along a horizontal line, color changes are almost always accompanied by luminance changes, and, since the bandwidth of the lumi-

nance is much higher than that of the chrominance, the effect of chrominance distortions will be secondary. With regard to luminance changes, three different waveforms are used to demonstrate the difference between the two prediction algorithms. The first waveform considered is the standard $2T$ pulse[2] shown in Fig. 3. This is a sine squared function, and is assumed repetitive from line-to-line. Calculations were done with a computer using the same general approach as shown in Appendices A and B. The results in Fig. 4 show that $XDIF_2$ (dotted line) has a reduced amplitude for both positive and negative directional peaks. In addition, the negative peaks are of shorter duration, resulting in less energy. Although this implies a slightly higher bandwidth, the magnitude of the band-limited signal for $XDIF_2$ is substantially less, indicating a more accurate reconstructed signal in the receiver, with less dependence on the differential signal.

The next waveform considered is the rising edge of the standard bar pulse[2] shown in Fig. 5. This function is represented a follows:

$$f(t) = \begin{cases} 0 & t < 0 \\ 6.4 \cdot 10^6 t & 0 \leq t \leq 156.25 \text{ ns} \\ 1 & t > 156.25 \text{ ns.} \end{cases}$$

Again, line-to-line repetition is assumed, and Fig. 6 shows the response of the two different algorithms. It can be seen that although the amplitudes of both differential signals are the same, the width is less for $XDIF_2$, resulting in less energy. Since the line-differential

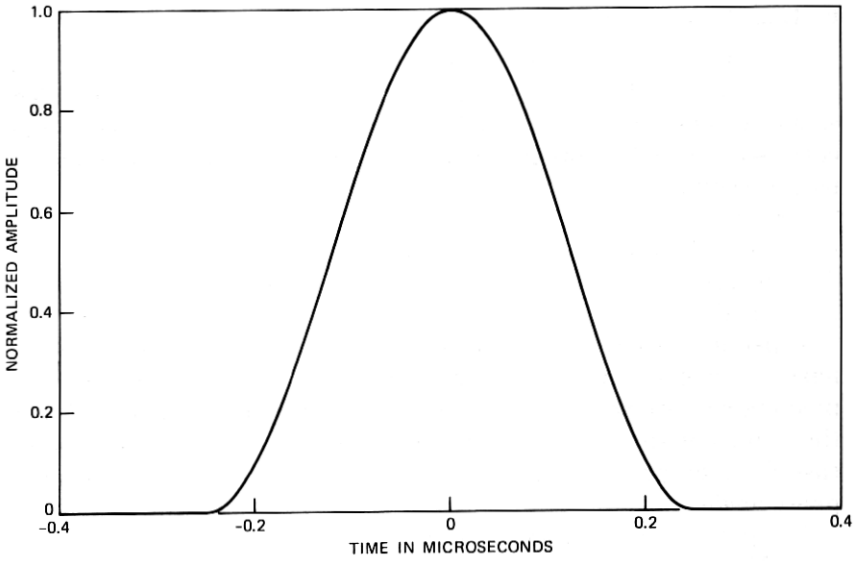

Fig. 3—Waveform of sine squared ($2T$) pulse from NTSC signal generator.

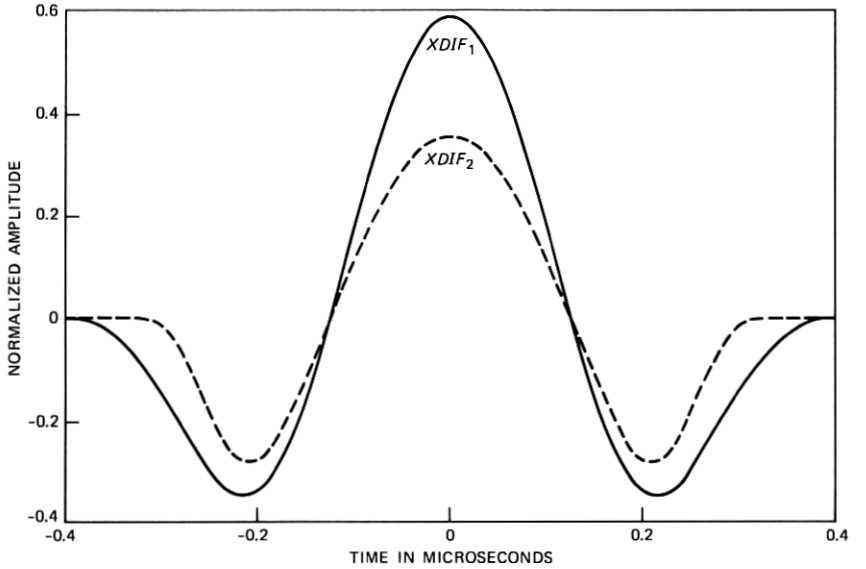

Fig. 4—Differential signal response of both algorithms to sine squared pulse.

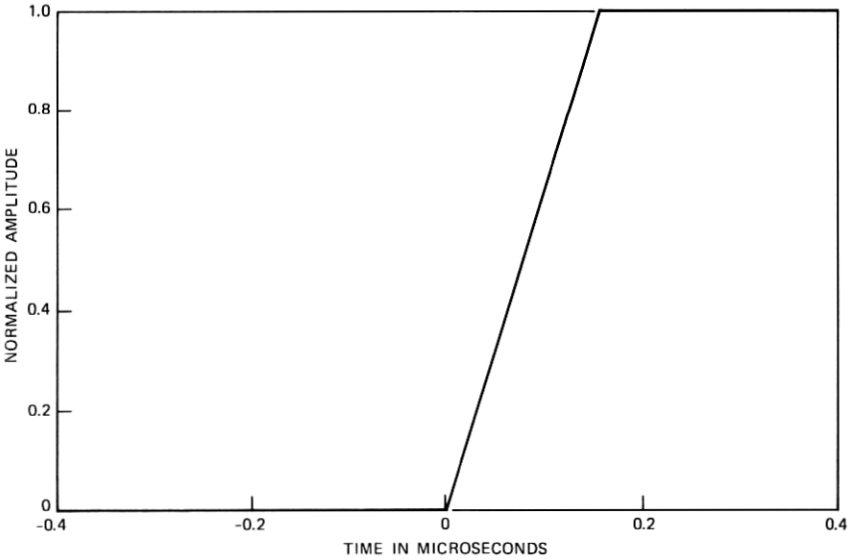

Fig. 5—Rising edge of bar pulse from NTSC signal generator.

signal in the proposed system is band limited to 3 MHz, this will again result in a smaller signal after filtering, with the same advantages as in the previous example.

The next and final waveform evaluated is a raised cosine function

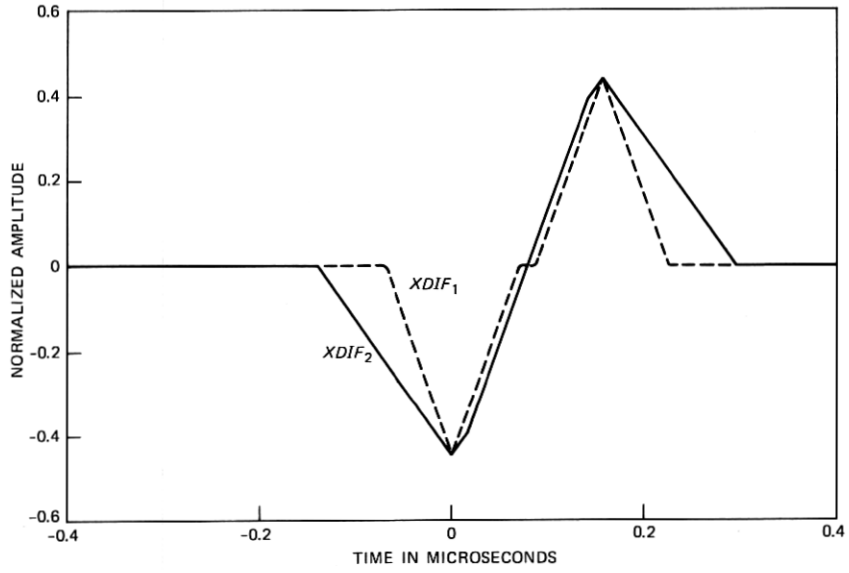

Fig. 6—Differential signal response of both algorithms to rising edge of bar pulse.

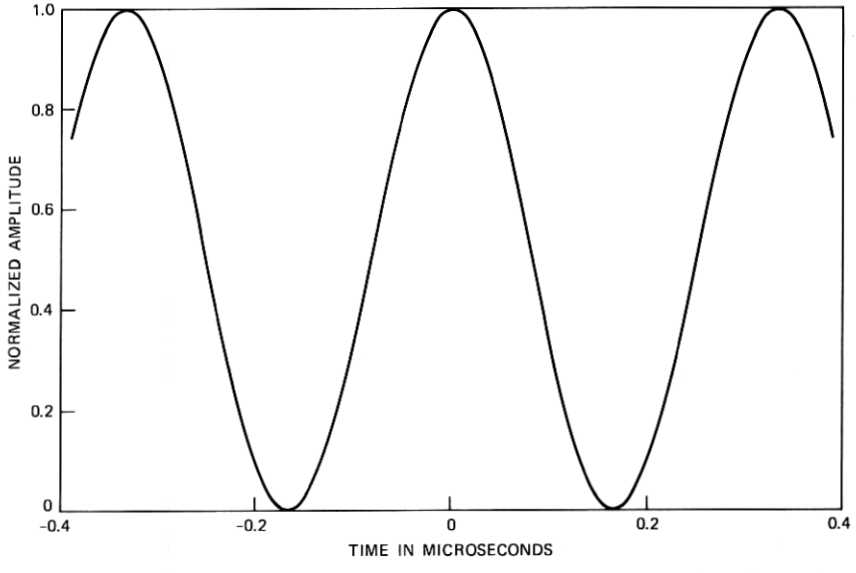

Fig. 7—Raised 3-MHz cosine demonstrating response of both algorithms to 3-MHz section of multiburst test signal.

at a frequency of 3 MHz, shown in Fig. 7. We chose this frequency because it is the intended maximum bandwidth of the differential signal. This would correspond to the fourth burst of the standard multiburst pattern[2] except that, for convenience, the amplitude is set to unity. Again, line-to-line repetition of the signal was assumed, and it can be seen in Fig. 8 that there is a 20-percent decrease in signal amplitude with $XDIF_2$. This again indicates a better reconstruction of the signal in the receiver with the available full bandwidth information.

III. FREQUENCY DOMAIN ANALYSIS

Before going into the analysis of the two predictors in the frequency domain, it will be useful to look at the frequency spectrum of a typical video signal.

It is well known[3] that the energy of a typical video luminance signal is concentrated on the harmonics of the horizontal or line sweep frequency F_H ($\approx$15734 Hz). This means that most of the luminance energy of the video signal is distributed at multiples of F_H along the frequency axis. The chrominance information also peaks at line frequency intervals, and, by placing the color subcarrier F_c at an odd multiple of half the line frequency, i.e., $F_c = 455/2 \cdot F_H$, the chrominance information will be interleaved with luminance information peaks.

Chrominance information bandwidth is approximately 1.5 MHz, but, with the composite signal band-limited to 4.2 MHz, it results in

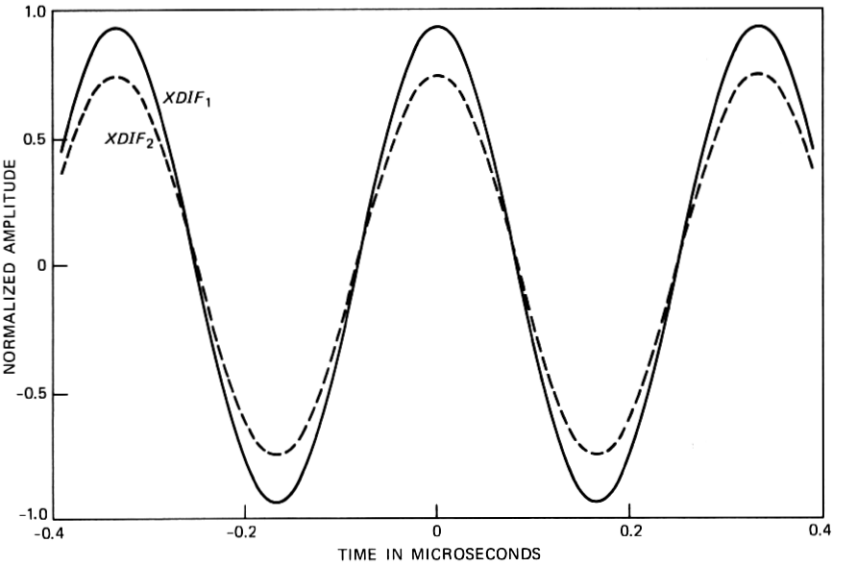

Fig. 8—Differential signal response of both algorithms to 3-MHz raised cosine.

a chrominance bandwidth of 1.5 MHz below the color subcarrier and 0.5 MHz above. Figure 9 shows the spectrum of a chrominance-modulated linear ramp test pattern. Figure 9a is the 0- to 4-MHz spectrum that shows the luminance information at low frequencies and the chrominance centered about $F_c = 3.579 \cdots$ MHz. Figure 9b shows the fundamental and the first nine harmonics of the line frequency, and Fig. 9c shows the color subcarrier and the line multiples on either side of it. It can be seen in this third photograph, also, that the luminance information (which peaks halfway between the chrominance peaks) is much lower than the chrominance at this frequency for this waveform.

The ideal frequency response of the linear system that produces the differential signal would then require that the differential signal be zero at even intervals of half the line frequency for the lower frequencies, and zero at odd intervals of half the line frequency for frequencies around the color subcarrier. Where the transition from odd to even intervals of half the line frequency should occur is not exactly defined, but it should not be lower than the lowest chrominance component, i.e., color subcarrier frequency minus the chrominance bandwidth, or approximately 2.08 MHz. In fact, the ideal value is picture dependent and, more exactly, would depend on the relationship between the luminance high-frequency content and the chrominance information content.

IV. FREQUENCY DOMAIN COMPARISON

It is well known from circuit theory that, in a linear system with input $x(t)$, output $y(t)$, and impulse response $h(t)$,

$$Y(j\omega) = H(j\omega) \cdot X(j\omega),$$

where uppercase letters designate Fourier Transforms. Since the time relationship of the differential predictors is known, the frequency domain representation of the network $H(j\omega)$ can be found easily, and this process is shown in Appendix C for both the original and the new predictors.

With the results of these simple calculations, a program was written to plot the network response $|H(j\omega)|$. Figures 10 and 11 show the 0- to 100-kHz response of the original and new differential signal networks, respectively. It can be seen that both signals are zero for the line frequency and its harmonics. Since this is where most of the incoming signal energy is concentrated, both of these algorithms should behave well in this regard.

Figures 12 and 13 show the response of the two algorithms in a 100-kHz interval centered around the color subcarrier. It can be seen that both algorithms are zero at the color subcarrier and are again periodic

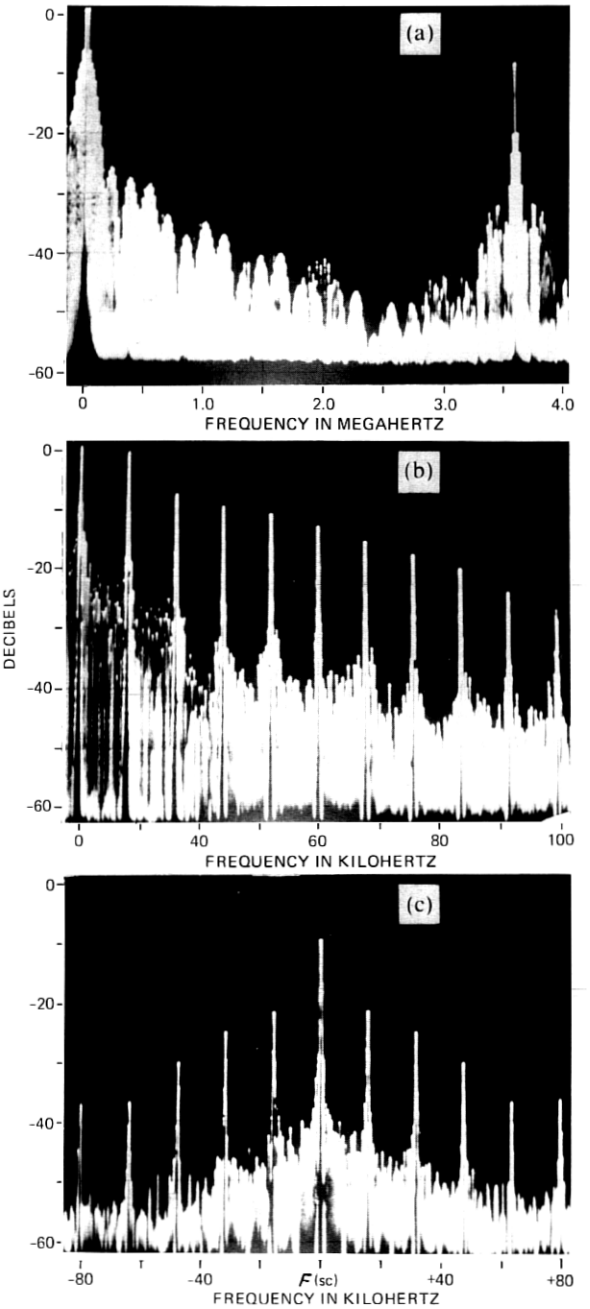

Fig. 9—Spectrum of chrominance-modulated linear ramp test pattern: (a) from 0 to 4.2 MHz; (b) from 0 to 100 kHz, with peaks at even multiples of half the line frequency; and (c) over a 100-kHz band centered around color subcarrier, with peaks at odd multiples of half the line frequency.

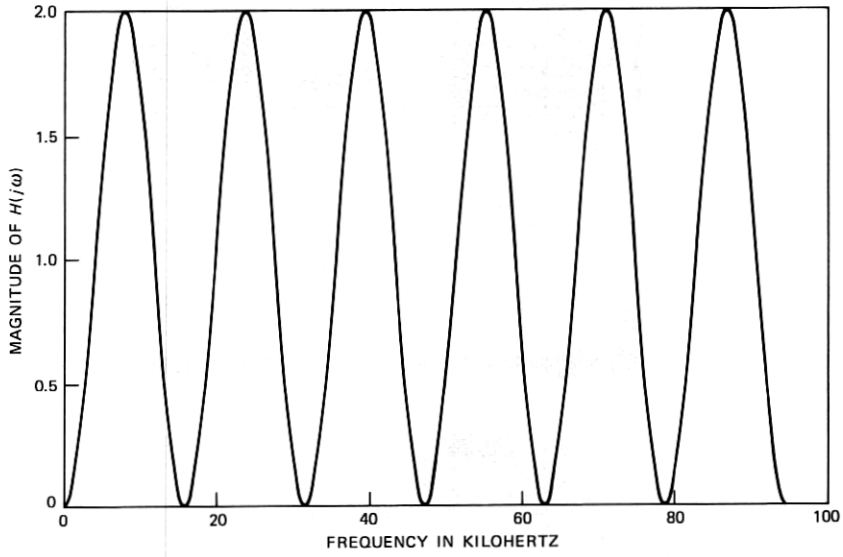

Fig. 10—Calculated differential signal spectrum of XP_1 algorithm from 0 to 100 kHz.

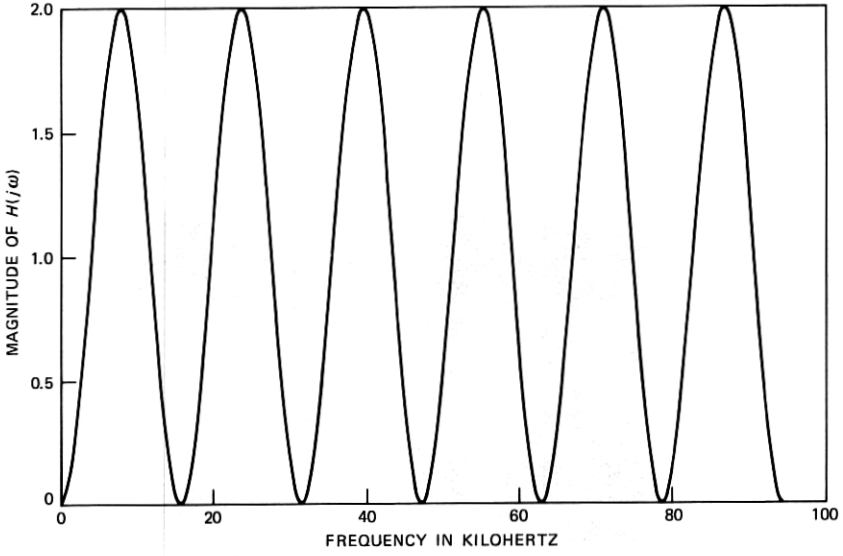

Fig. 11—Calculated differential signal spectrum of XP_2 algorithm from 0 to 100 kHz.

at a line rate. Since this corresponds to the high-energy chrominance portions of the incoming signal for this part of the spectrum, both algorithms should again behave well.

The difference in the response of the two algorithms can be seen,

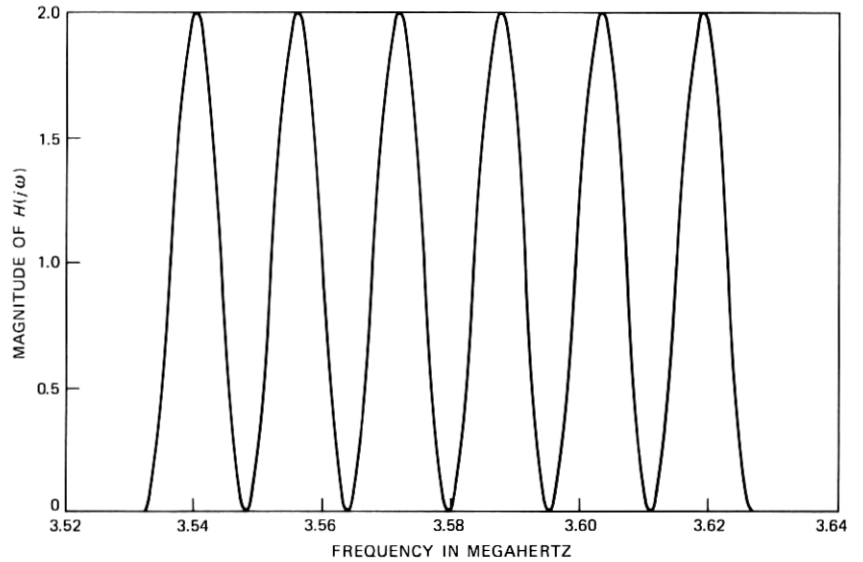

Fig. 12—Calculated differential signal spectrum of XP_1 algorithm for 100-kHz window centered around color subcarrier.

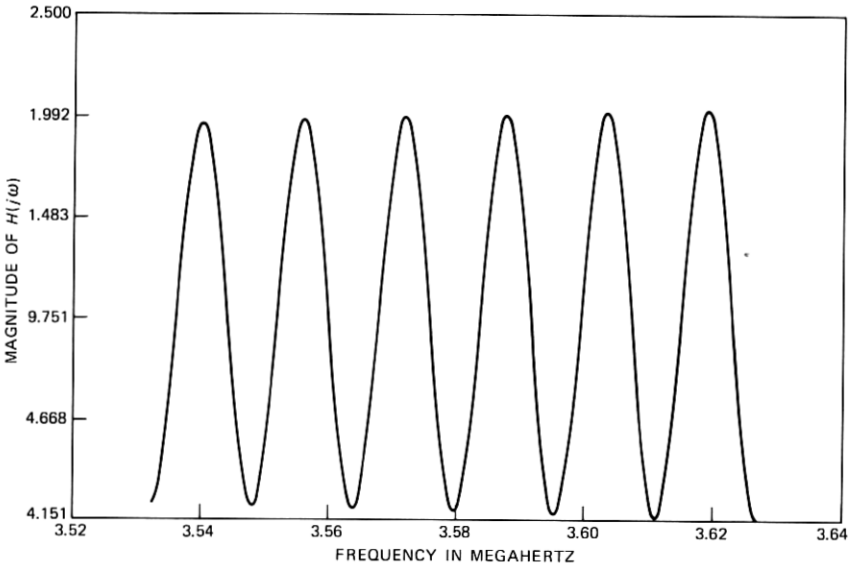

Fig. 13—Calculated differential signal spectrum of XP_2 algorithm for 100-kHz window centered around color subcarrier.

however, in Figs. 14 and 15. In these figures the differential signal response is plotted from 0 to 3 MHz, and the oscillatory response pattern is shown with the sine wave minimum values falling on even multiples of half the line frequency in the lower part of the spectrum, and at odd multiples of half the line frequency in the upper part.

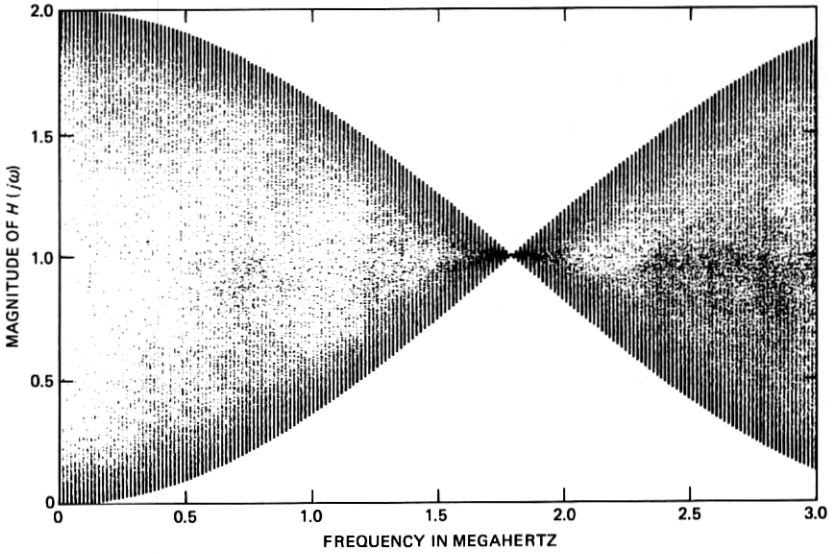

Fig. 14—Calculated differential signal spectrum of XP_1 algorithm from 0 to 3 MHz.

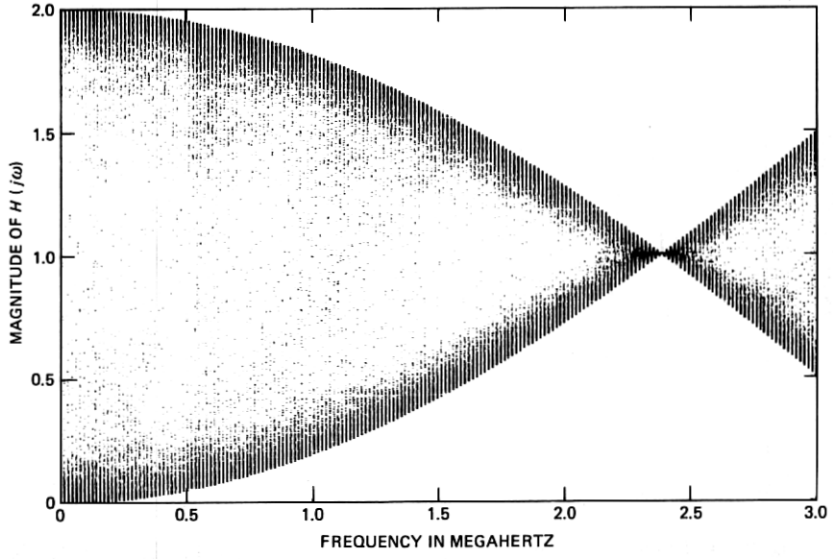

Fig. 15—Calculated differential signal spectrum of XP_2 algorithm from 0 to 3 MHz.

Because the lower limit of the chrominance information bandwidth is 2.08 MHz, we can see that the $XDIF_1$ transition is too soon (at about 1.8 MHz). This results in a greater than unity gain for the luminance information in this region and, therefore, a poorer prediction with no resulting savings in chrominance information because it is out of band. The $XDIF_2$ signal, however, is below unity for luminance response until 2.38 MHz, giving a better luminance prediction over an additional 500 kHz of bandwidth. This gives a poorer line difference prediction for the upper 300 kHz of the chrominance band, but since a fast chrominance change is almost always accompanied by a luminance change, the loss should be offset by an improvement in luminance response. Figure 16 plots the envelope for the luminance response and shows that the $XDIF_2$ signal will be lower throughout this whole region, indicating a better line difference prediction. These plots cross over at the color subcarrier, but that is of no concern since the differential signal will be band limited to 3 MHz in the proposed system.

V. HARDWARE VERIFICATION OF RESULTS

To verify these results, a Tektronix test signal generator was modified so that a sweep generator signal could be added to the flat field test pattern. In this way the system could be analyzed with a full field sine wave input. The differential signal was then put into a spectrum

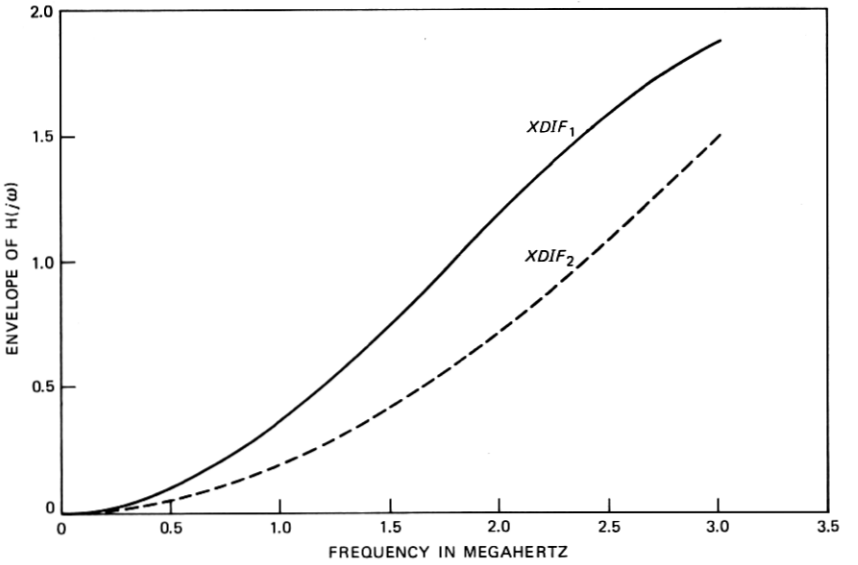

Fig. 16—Envelope of differential signal frequency response for XP_1 and XP_2, with samples taken at even multiples of half the line frequency.

analyzer. Figure 17 shows photographs of the 0- to 100-kHz spectrum and the 0- to 3-MHz spectrum. The response of the network is identical to the computed values shown in Figs. 10 through 16.

Time domain measurements were also made to verify the results of the analysis of this paper. The measurements were made with the full field pulse bar test pattern from the NTSC test signal generator. The differential signal output was band limited to 3 MHz, which resulted in some deviation from the calculated ideal results. Figures 18a and 18b show the response of the two algorithms to the sine squared pulse. A slight spreading of the signal caused by filtering can be seen, but otherwise the results are quite close to the ideal calculations. Figures 18c and 18d then show the response to the 156.25-ns ramp (bar pulse). Here again the high resolution of the ideal waveforms is lost because of filtering, but the predicted decrease in amplitude is clear.

Subjective tests were then carried out to determine if any degradation in picture quality was visible with either line difference prediction

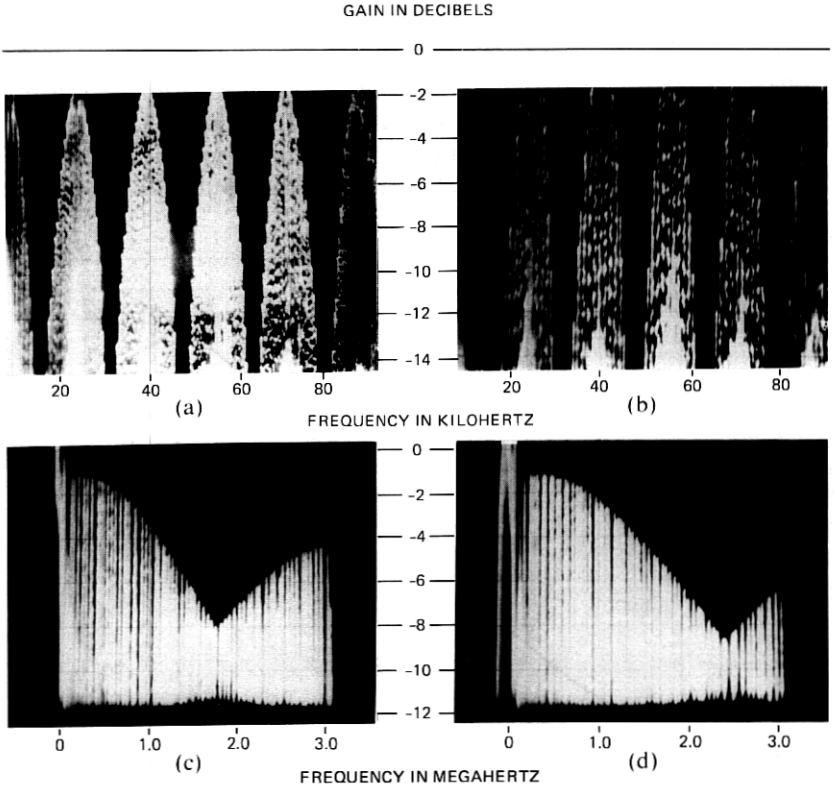

Fig. 17—Measured differential signal frequency responses of algorithms: (a) XP_1 from 0 to 100 kHz, (b) XP_2 from 0 to 100 kHz, (c) XP_1 from 0 to 3 MHz, and (d) XP_2 from 0 to 3 MHz.

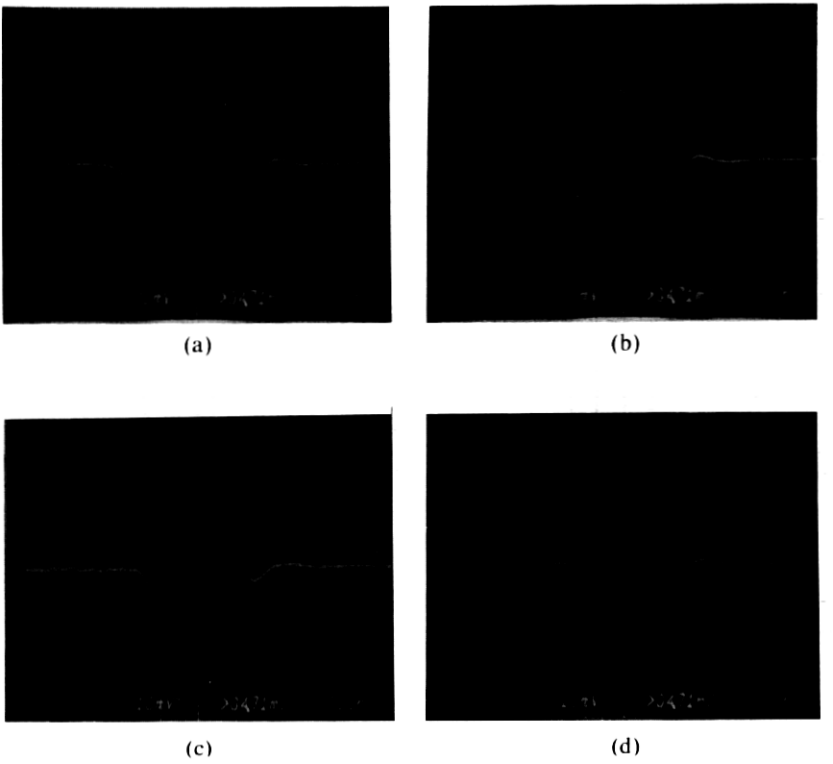

Fig. 18—Measured differential signal time domain responses of both algorithms to the sine for (a) XP_1 and (b) XP_2. Same responses to rising edge of the bar pulse for (c) XP_1 and (d) XP_2.

algorithm. To minimize distortion contributions from other hardware sources, so that contributions from the algorithm would be the primary cause of degradation, the TFM hardware was simplified. The band-limited differential signal and the time-multiplexed baseband signals from the transmitter were sent on individual coaxial cables to the receiver. This avoided signal degradations from the frequency multiplexing operation, and also transmission system degradations, leaving only the analog baseband amplifiers and two analog-to-digital-to-analog conversions as additional sources of degradation. Both the transmitter and the receiver use eight-bit pulse code modulation (PCM) for their digital processing, so that these additional contributions should be small in comparison with the differential signal band limiting. A block diagram of the test configuration is shown in Fig. 19.

Several video signals were evaluated using a stringent comparison between the reconstructed video signals and one which is unimpaired except for the two analog-to-digital conversions. The signals were switched on the same television monitor during the vertical blanking

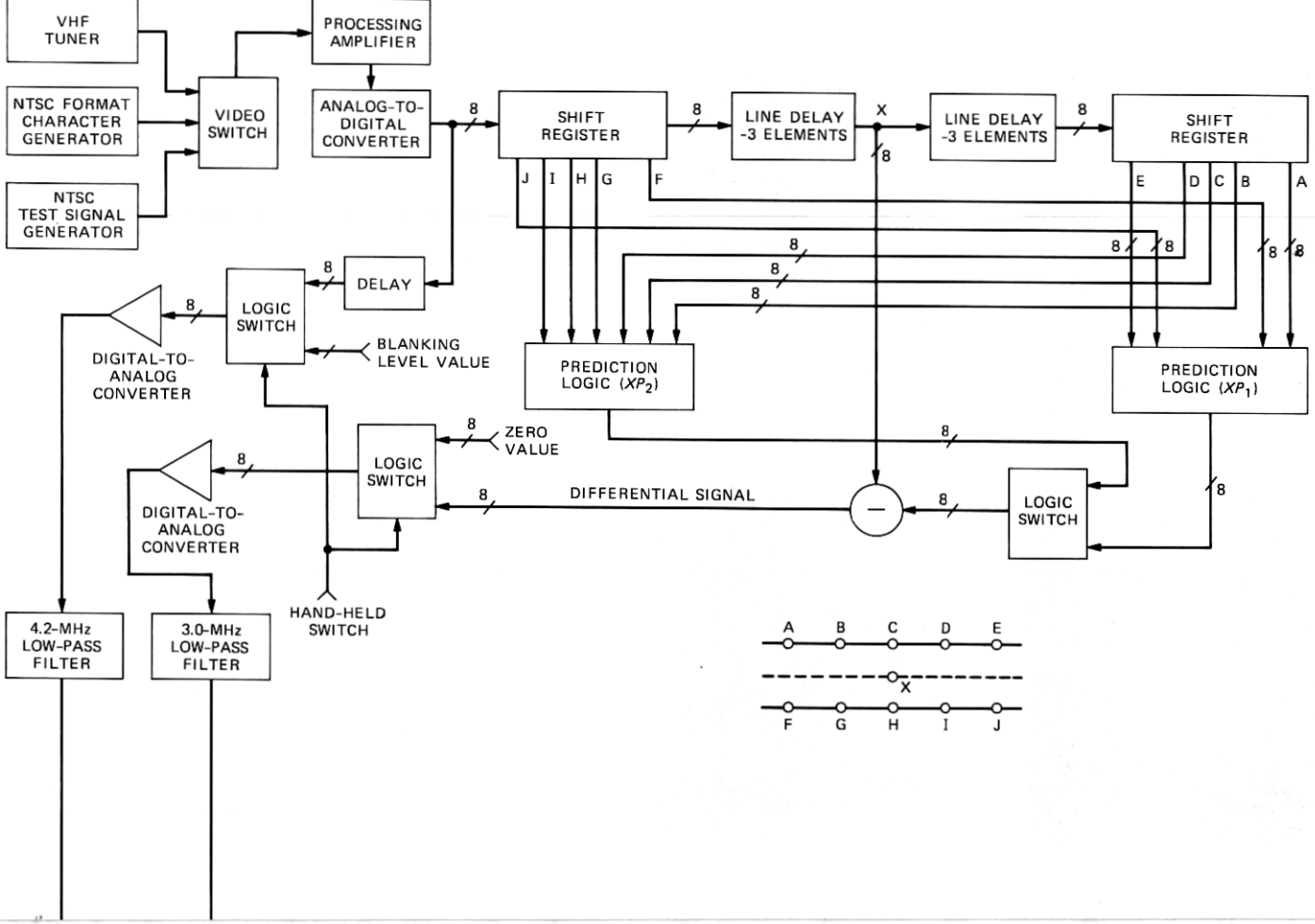
VHF TUNER
PROCESSING AMPLIFIER
NTSC FORMAT CHARACTER GENERATOR
VIDEO SWITCH
ANALOG-TO-DIGITAL CONVERTER
NTSC TEST SIGNAL GENERATOR
SHIFT REGISTER
LINE DELAY -3 ELEMENTS
LINE DELAY -3 ELEMENTS
SHIFT REGISTER
J I H G F
E D C B A
DELAY
LOGIC SWITCH
BLANKING LEVEL VALUE
DIGITAL-TO-ANALOG CONVERTER
PREDICTION LOGIC (XP_2)
PREDICTION LOGIC (XP_1)
ZERO VALUE
LOGIC SWITCH
DIFFERENTIAL SIGNAL
LOGIC SWITCH
DIGITAL-TO-ANALOG CONVERTER
HAND-HELD SWITCH
4.2-MHz LOW-PASS FILTER
3.0-MHz LOW-PASS FILTER
A B C D E
X
F G H I J

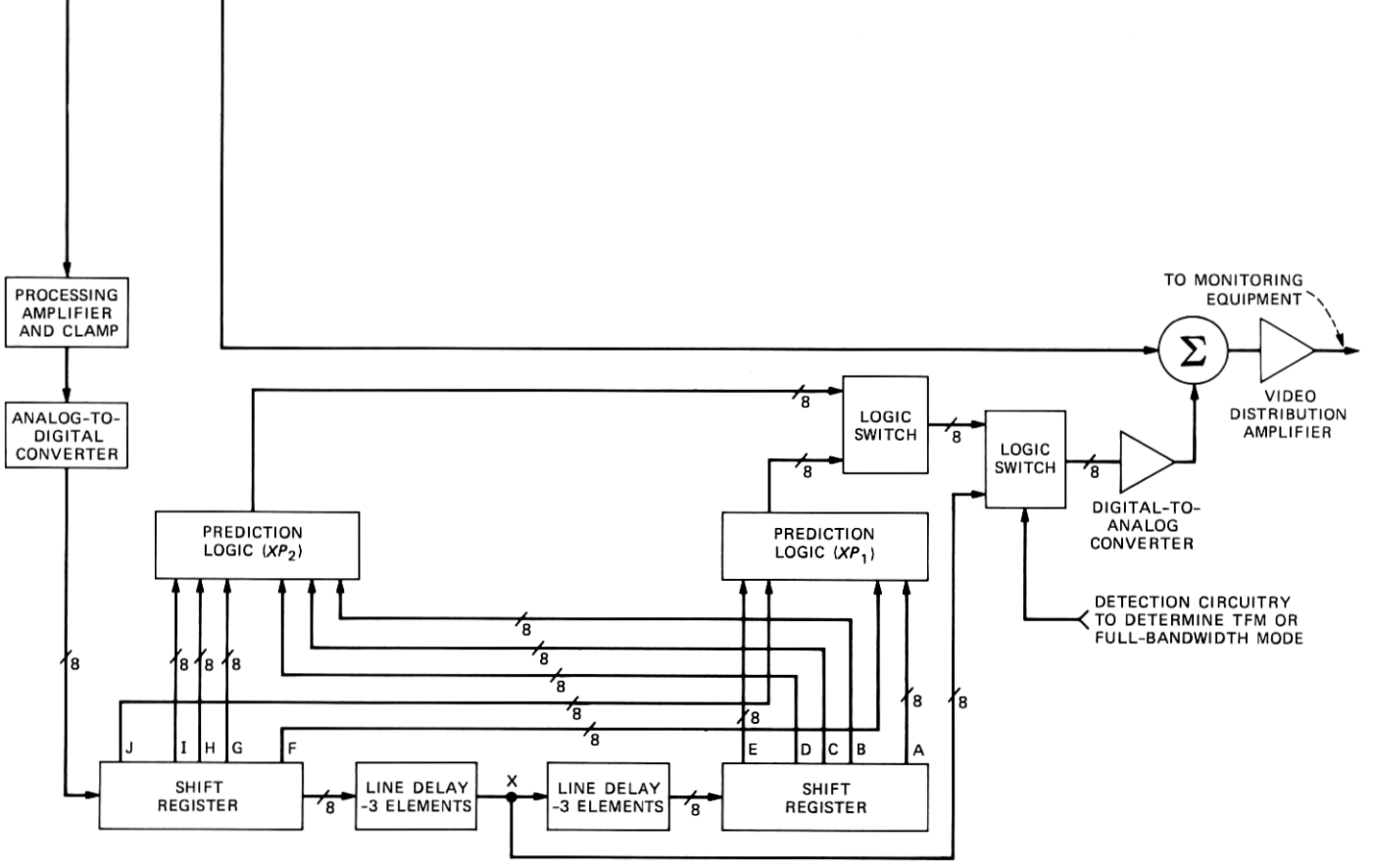

Fig. 19—Block diagram of test configuration used to elevate prediction algorithms.

intervals so that switching transitions were only visible when coding caused degradation. A toggle switch in both the transmitter and receiver allowed selection of either algorithm. The television monitor used for this evaluation did not contain a comb filter, so there is a possibility that some degradation caused by coding was masked by the luminance component band limiting. However, since both algorithms were evaluated with the same constraints, this did not appear to be a problem.

Results showed that with normal off-the-air video signals both algorithms performed well, and neither one produced any visible degradation. However, with electronically generated test patterns and text, the degradation of high-frequency signals, such as the $2T$ pulse, the multiburst pattern, and character edges, was less severe with the new algorithm.

VI. CONCLUSIONS

Subjective tests verified the results of this analysis. Thus, the quality of a picture using the band-limited differential signal is improved with the new algorithm. The implementation is somewhat more difficult than the original one and requires only the addition of two more arithmetic stages. It is, therefore, a practical and desirable change to make in the system.

REFERENCES

1. B. G. Haskell, "Time-Frequency Multiplexing (TFM) of Two NTSC Color TV Signals—Simulation Results," B.S.T.J., *60*, No. 5 (May–June 1981), pp. 643–660.
2. *NTC Report No. 7, Video Facility Testing Technical Performance Objectives*, June 1975, revised January 1976. Published by Public Broadcasting Service.
3. D. Fink, *Television Engineering Handbook*, New York: McGraw-Hill, 1957.

APPENDIX A

Comparison of Differential Signal Responses to a Constant Color, Flat Field Luminance Video Signal

Consider a uniform flat field of some color for the XP_1 algorithm shown in Fig. 1:

$$XDIF_1 = X - 1/4(A + E + F + J).$$

Let $X = U\cos(2\pi F_c t)$, where F_c = the color subcarrier frequency. Then, since it is a uniform flat field,

$$A = E = F = J = U\cos(2\pi F_c t) = X.$$

Therefore,

$$XDIF_1 = 0 \qquad \text{for all } t.$$

For the XP_2 prediction shown in Fig. 2 with the same X as above,

$$XDIF_2 = X - [1/2(B + D + G + I) - 1/2(C + H)].$$

Letting $\omega_c = 2\pi F_c$ we have

$$B = G = U \cos\left(\omega_c t + \frac{\pi}{2}\right),$$

$$D = I = U \cos\left(\omega_c t - \frac{\pi}{2}\right),$$

and

$$C = H = U \cos(\omega_c t + \pi);$$

therefore

$$\begin{aligned} XDIF_2 &= U \cos(\omega_c t) - \frac{U}{2}\left[2 \cos\left(\omega_c t + \frac{\pi}{2}\right)\right. \\ &\qquad \left. + 2 \cos\left(\omega_c t - \frac{\pi}{2}\right) + 2 \cos(\omega_c t)\right] \\ &= U \cos(\omega_c t) - U[-\sin(\omega_c t) + \sin(\omega_c t) + \cos(\omega_c t)] \\ &= U \cos(\omega_c t) - U \cos(\omega_c t) \\ &= 0 \qquad \text{for all } t. \end{aligned}$$

APPENDIX B

Comparison of Differential Signal Responses to an Adjacent Line Color Change, Flat Field Luminance Video Signal

Now consider a color change with no corresponding luminance change from one line to the next. The change will be considered between lines two and three of the prediction area, although calculations would be identical for a change from line one to two. Let U = magnitude of the first color, V = magnitude of the second color, and $\omega_c = 2\pi F_c$. Then for the XP_1 predictor,

$$\begin{aligned} XDIF_1 &= U \cos(\omega_c t) - \left[\frac{U}{2} \cos(\omega_c t) + \frac{V}{2} \cos(\omega_c t + \phi)\right] \\ &= \frac{U}{2} \cos(\omega_c t) - \frac{V}{2} \cos(\omega_c t + \phi), \end{aligned}$$

where the worst case would be for $\phi = \pi$, giving

$$XDIF_1 = \frac{U + V}{2} \cos(\omega_c t).$$

For the XP_2 predictor,

$$XDIF_2 = U\cos(\omega_c t) - \frac{1}{2}\left[U\cos\left(\omega_c t + \frac{\pi}{2}\right) + U\cos\left(\omega_c t + \frac{\pi}{2}\right) + V\cos(\omega_c t + \phi) + V\cos(\omega_c t + \pi + \phi) - U\cos(\omega_c t + \pi) - V\cos\left(\omega_c t + \frac{\pi}{2} + \phi\right)\right]$$

$$= U\cos(\omega_c t) - \frac{1}{2}[V\cos(\omega_c t + \phi) - V\cos(\omega_c t + \phi) + U\cos(\omega_c t) + V\sin(\omega_c t + \phi)]$$

$$= U\cos(\omega_c t) - \frac{U}{2}\cos(\omega_c t) - \frac{V}{2}\sin(\omega_c t + \phi)$$

$$= \frac{U}{2}\cos(\omega_c t) - \frac{V}{s}\sin(\omega_c t + \phi),$$

where the worst case will occur when $\sin(\omega_c t + \phi)$ equal $-\cos(\omega_c t)$ or at ϕ equal to $-\frac{\pi}{2}$, giving

$$XDIF_2 = \frac{U + V}{2}\cos(\omega_c t),$$

which is the same as for $XDIF_1$.

APPENDIX C

Transfer Function Derivation for Both Prediction Algorithms

Knowing the time relationship of the picture elements, we can find the Fourier Transform of the impulse responses of the differential signal algorithms. Let $p = 1$ picture element with a duration of $6.98412 \cdot 10^{-8}$ second. Then $910p = 1$ line $= 6.3555 \cdot 10^{-5}$ second.

For the XP_1 predictor:

$$XDIF_1(t) = X(t) - \frac{1}{4}[X(t + 908p) + X(t + 912p) + X(t - 908p) + X(t - 912p)],$$

$$XDIF_1(j\omega) = X(j\omega) - \frac{1}{4}[X(j\omega)e^{-j\omega 908p} + X(j\omega)e^{-j\omega 912p} + X(j\omega)e^{+j\omega 908p} + X(j\omega)e^{j\omega 912p}]$$

$$= X(j\omega)\left\{1 - \frac{1}{4}\left[e^{908pj\omega} + e^{-908pj\omega} + e^{912pj\omega} + e^{-912pj\omega}\right]\right\}$$

$$= X(j\omega)\left\{1 - \frac{1}{2}\left[\cos(908p\omega) + \cos(912p\omega)\right]\right\}$$

$$= X(j\omega)\cdot H(j\omega),$$

with

$$H(j\omega) = 1 - \tfrac{1}{2}[\cos(908p\omega) + \cos(912p\omega)].$$

Now for the XP_2 predictor:

$$\begin{aligned} XDIF_2(t) &= X(t) - \{1/2[X(t-911p) + X(t-909p) + X(t+909p) \\ &\quad + X(t+911p)] - 1/2[X(t-910p) + X(t+910p)]\}, \\ XDIF_2(j\omega) &= X(j\omega) - \{1/2[X(j\omega)e^{+911pj\omega} + X(j\omega)e^{+909pj\omega} \\ &\quad + X(j\omega)e^{-909pj\omega} + X(j\omega)e^{-911pj\omega}] \\ &\quad - [X(j\omega)e^{910pj\omega} + X(j\omega)e^{-910pj\omega}]\} \\ &= X(j\omega)\{1 - [(e^{909pj\omega} + e^{-909pj\omega}/2) + (e^{911pj\omega} + e^{-911pj\omega}/2) \\ &\quad - (e^{910pj\omega} + e^{-910pj\omega}/2)]\} \\ &= X(j\omega)\{1 - [\cos(909pj\omega) + \cos(911pj\omega) - \cos(910pj\omega)]\}. \end{aligned}$$

Therefore,

$$H(j\omega) = 1 + \cos(910pj\omega) - \cos(909pj\omega) - \cos(911pj\omega).$$

AUTHOR

Robert L. Schmidt, B.S.E.E., 1982, Monmouth College; Bell Laboratories, 1972—. Mr. Schmidt is currently a member of the Radio Communications Research Department, where he has been exploring various techniques in combining multiple television signals onto a single analog radio channel. He has researched television signal encoding, bit rate reduction techniques, and software-controlled coding systems. Member, Eta Kappa Nu.